Synchronized states in a ring of mutually coupled self-sustained electrical oscillators

P. Woafo*
Laboratoire de Mécanique, Faculté des Sciences, Université de Yaoundé I, Boîte Postale 812, Yaoundé, Cameroon

H. G. Enjieu Kadji
Institut de Mathématiques et de Sciences Physiques, Boîte Postale 613, Porto-Novo, Bénin

(Received 2 September 2003; published 29 April 2004)

We investigate in this paper different states of synchronization in a ring of mutually coupled self-sustained electrical oscillators. The good coupling parameters leading to complete and partial synchronization or disordered states are calculated using the properties of the variational equations of stability. A stability map showing domains of synchronization to an external excitation locally injected in the ring is also obtained. In both cases, the numerical simulation validates and complements the results of the analytical investigation.

DOI: 10.1103/PhysRevE.69.046206 PACS number(s): 05.45.Gg

I. INTRODUCTION

For many years, synchronization of coupled oscillators has been investigated by the scientific community. The main reason for this growing interest is that synchronization is frequent in nature and can help to explain many phenomena in biology, chemistry, physics, or has potential applications in engineering and communication [1–7]. In the majority of cases, two types of behaviors are of interest: chaotic and relaxation.

For the first type, complete synchronization of chaotic oscillators has been described theoretically and observed experimentally. Zhang *et al.* (see Ref. [8] and references therein) have studied partial synchronization and spatial ordering in Rössler oscillators. They have investigated the stability of different partially synchronous spatiotemporal structures and some dynamical behaviors of these states have been discussed using numerical and analytical investigations. Recently, Chembo and Woafo [9,10] studied the spatiotemporal dynamics of a ring of diffusely coupled single-well Duffing oscillators with a positive nonlinear stiffness coefficient. They used the Floquet theory to investigate various dynamical states of the ring as well as the Hopf bifurcations between them and applied the local injection method to recover the chaotic dynamics.

For the second type, Somers and Kopell [11] showed that a ring of identical relaxation oscillators, coupled locally in a manner that mimics fast excitatory synapes, can lead to synchronization within a couple of cycles. They also showed why relaxation oscillators can more robustly encode domains of synchrony [12].

Recently, Ookawara and Endo [13] have investigated the effect of element value deviation on the degenerate modes in a ring of three and four coupled Van der Pol oscillators. By using the averaging method, they proved that for a ring of three coupled oscillators, two frequencies bifurcate from the degenerate mode, synchronize if they are close enough, but lose synchronization when they are separated to some extent; while for a ring of four coupled oscillators, the two frequencies generally cannot be synchronized, even if they are close enough.

The purpose of this paper is to consider the synchronized states in a ring of mutually coupled self-sustained electrical oscillators described by coupled Van der Pol equations. We first analyze the stability of the synchronization of the ring using analytical and numerical investigations. Then, we find the effects of the local injection strength on the behavior of the ring. After presenting the physical model in the next section, we analyze in Sec. III the stability of the synchronization in the ring using the Floquet theory and Whittaker method. In Sec. IV, the influence of a local injection is found. The last section is devoted to the conclusion.

II. MODEL AND STATEMENT OF THE PROBLEM

The model shown in Fig. 1 is a ring of N identical mutually coupled self-excited electrical circuits described by coupled Van der Pol oscillators (see Fig. 2). Each oscillator consists of a nonlinear resistor NR, an inductor L, and a condenser C, all connected in parallel. The coupling between the N identical oscillators is realized here through an inductor L_c (low-pass oscillators), but can also be done with a

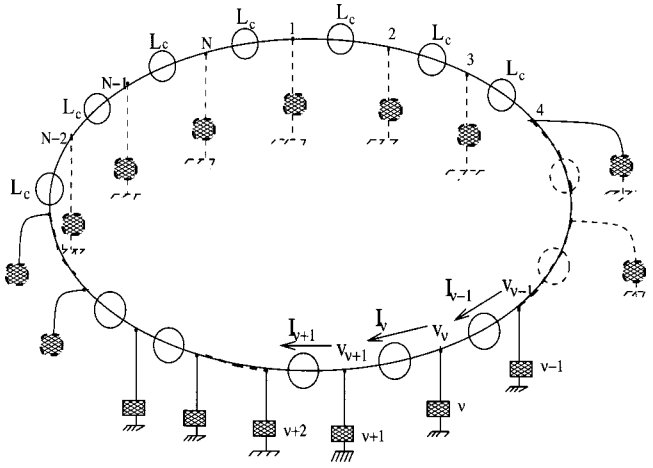

FIG. 1. Ring of N mutually coupled self-sustained electrical oscillators.

*Email address: pwoafo@uycdc.uninet.cm

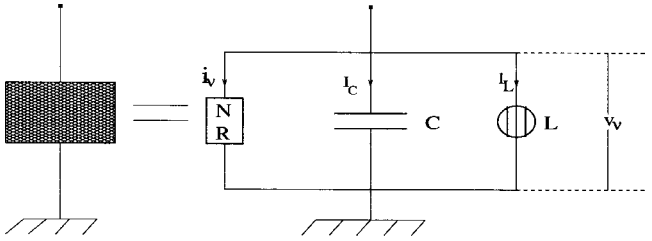

FIG. 2. A self-sustained electrical oscillator.

capacitor (high-pass oscillators). The volt-ampere characteristic of the nonlinear resistor for the νth unit is expressed by a symmetric cubic nonlinearity, which is illustrated by

$$i_\nu = -a_1 V_\nu + a_3 V_\nu^3, \quad a_1, a_3 > 0; \quad \nu = 1,2,...,N. \tag{1}$$

In this case, the model has the property to exhibit self-excited oscillations. This is due to the fact that the model incorporates through its nonlinear resistance a dissipative mechanism to damp oscillations that grow too large and a source of energy to pump up those that become too small. This form of nonlinearity was introduced by Van der Pol, who considered a lumped oscillator with two degrees of freedom to discuss simultaneous multimode oscillations [14,15].

As we have shown in the Appendix, the model is described by the following second-order nondimensional nonlinear differential equations:

$$\begin{aligned}
&\ddot{x}_1 - \mu(1-x_1^2)\dot{x}_1 + x_1 = K(x_2 - 2x_1 + x_N),\\
&\ddot{x}_\nu - \mu(1-x_\nu^2)\dot{x}_\nu + x_\nu = K(x_{\nu+1} - 2x_\nu + x_{\nu-1}),\\
&\qquad \vdots \quad \vdots \quad \vdots \quad \vdots \quad \vdots\\
&\ddot{x}_N - \mu(1-x_N^2)\dot{x}_N + x_N = K(x_1 - 2x_N + x_{N-1}),
\end{aligned} \tag{2}$$

where $\nu = 2,...,N-1$ and the dot over a quantity denotes the time derivative. x_ν stands for the amplitude of the voltage at the νth oscillator, μ is a positive coefficient, and K is the coupling parameter. The equations of motion (2) are a set of N identical coupled Van der Pol or self-sustained oscillators.

Equations (2) are interesting because they model several phenomena and have applications in many areas. In that channel, this model is mainly used in electronics engineering as a network of parallel microwave oscillators [16,17]. Such a network allows us to investigate the possibility of simultaneous multimode oscillations and accordingly the stability of several nonresonant modes of oscillations under specific boundary conditions (two modes are nonresonant if the ratio of their frequencies is an irrational number) [18]. In biology, the network of a large number of these oscillators can be used to model intestinal signal [19] or colorectal myoelectrical activity in humans [20]. Moreover, the central pattern generator (CPG) that controls the rhythmic activity in invertebrates can be modeled by the same system [21]. It can also be used to investigate the stability of both nondegenerate modes (standing waves) and degenerate modes (traveling waves), and in particular the existence of an irregular degenerate mode that appears when the number N of oscillators is a multiple of 4 [22].

III. SYNCHRONIZATION ANALYSIS IN THE RING

A. Analytical treatment

A particular property of the Van der Pol oscillator whose final state is a sinusoidal limit cycle or relaxation oscillations [14,15] is the sensibility of its phase to initial conditions. Consequently, if N identical Van der Pol oscillators are launched with different initial conditions, they will circulate on the same limit cycle but with N different phases. The aim of the synchronization is therefore to phase-lock those oscillators (phase synchronization). When the oscillators are coupled as in Eqs. (2), the resulting dynamical state of the system is interesting when it is stable. This requires that all the perturbed trajectories return to the original limit cycle. But for the sake of exemplification, we set N to 4. Thus, the stability of the dynamical state can be studied through the linearization of Eqs. (2) around the unperturbed limit cycle (or orbit) x_o according to

$$\begin{aligned}
&\ddot{\xi}_1 - \mu(1-x_o^2)\dot{\xi}_1 + (1 + 2K + 2\mu x_o \dot{x}_o)\xi_1 = K(\xi_2 + \xi_4),\\
&\ddot{\xi}_2 - \mu(1-x_o^2)\dot{\xi}_2 + (1 + 2K + 2\mu x_o \dot{x}_o)\xi_2 = K(\xi_1 + \xi_3),\\
&\ddot{\xi}_3 - \mu(1-x_o^2)\dot{\xi}_3 + (1 + 2K + 2\mu x_o \dot{x}_o)\xi_3 = K(\xi_2 + \xi_4),\\
&\ddot{\xi}_4 - \mu(1-x_o^2)\dot{\xi}_4 + (1 + 2K + 2\mu x_o \dot{x}_o)\xi_4 = K(\xi_1 + \xi_3),
\end{aligned} \tag{3}$$

where ξ_ν stands for the perturbation term. For small values of μ, the behavior of one oscillator can be described by a pure sinusoidal trajectory of the form

$$x_o = A\cos(\omega t - \varphi), \tag{4}$$

where A and ω are, respectively, the amplitude and the frequency of the unperturbed limit cycle in the first approximation. The values of A and ω are $A = 2.00$ and $\omega = 0.999$ for $\mu = 0.10$ (obtained, for instance, by the averaging method). As reported in Ref. [23] dealing with the synchronization of two Van der Pol oscillators, this first-order approximation gives fairly good agreement between the analytical and numerical results. If we introduce the rescaling $\tau = \omega t - \varphi$ and the following diagonal variables (or Fourier modes) ρ_i as

$$\begin{aligned}
\rho_1 &= \xi_1 + \xi_2 + \xi_3 + \xi_4,\\
\rho_2 &= \xi_4 - \xi_2 = x_4 - x_2,\\
\rho_3 &= \xi_3 - \xi_1 = x_3 - x_1,\\
\rho_4 &= \xi_4 - \xi_3 + \xi_2 - \xi_1 = x_4 - x_3 + x_2 - x_1,
\end{aligned} \tag{5}$$

we get, after some algebraic manipulation, the following variational equations:

$$\ddot{\rho}_i + [2\lambda + F(\tau)]\dot{\rho}_i + G_i(\tau)\rho_i = 0, \quad i = 1,2,3,4, \tag{6}$$

with

$$\lambda = -\frac{\mu}{2\omega}\left(1-\frac{A^2}{2}\right),$$

$$F(\tau) = \frac{\mu A^2}{2\omega}\cos 2\tau,$$

$$G_1(\tau) = \frac{1}{\omega^2}(1-\mu A^2\omega \sin 2\tau),$$

$$G_2(\tau) = G_3(\tau) = \frac{1}{\omega^2}(1+2K-\mu A^2\omega \sin 2\tau),$$

$$G_4(\tau) = \frac{1}{\omega^2}(1+4K-\mu A^2\omega \sin 2\tau).$$

From the expression of $G_2(\tau)$ and $G_3(\tau)$, we find that if $K \in]-\infty,-0.50[$, ρ_2 and ρ_3 will grow indefinitely, leading to the instability, in the ring. The same phenomenon also occurs for ρ_4 from the expression of $G_4(\tau)$ when $K \in]-\infty,-0.25[$ ($]a,b[$ means the internal from a to b but with a and b excluded). Taking the union of the two domains, this means that any perturbed trajectory in the region of $K \in]-\infty,-0.25[$ leads the oscillators to continuously drift away from their original limit cycles because the restoring force turns out to be repelling and the cycle loses its attraction character of the disturbed trajectory.

To discuss further the stability of the synchronization process, let us rewrite Eqs. (6) in a standard form. For this objective, we use the transformation

$$\rho_i = n_i \exp(-\lambda\tau)\exp\left(-\frac{1}{2}\int F(\tau')d\tau'\right) \tag{7}$$

and obtain that η_i satisfies the following set of independent Hill equations [24,25]:

$$\ddot{n}_i + (a_{0i} + 2a_{1s}\sin 2\tau + 2a_{1c}\cos 2\tau + 2a_{2c}\cos 4\tau)n_i = 0,$$
$$i = 1,2,3,4, \tag{8}$$

where

$$a_{01} = \frac{1}{\omega^2}\left[1-\frac{\mu^2}{4}\left(1-\frac{A^2}{2}\right)^2 - \mu^2\frac{A^4}{32}\right],$$

$$a_{02} = a_{03} = \frac{1}{\omega^2}\left[1+2K-\frac{\mu^2}{4}\left(1-\frac{A^2}{2}\right)^2 - \mu^2\frac{A^4}{32}\right],$$

$$a_{04} = \frac{1}{\omega^2}\left[1+4K-\frac{\mu^2}{4}\left(1-\frac{A^2}{2}\right)^2 - \mu^2\frac{A^4}{32}\right],$$

$$a_{1s} = -\frac{\mu A^2}{4\omega},$$

$$a_{1c} = \frac{\mu^2}{8\omega^2}\left(1-\frac{A^2}{2}\right)A^2,$$

$$a_{2c} = -\frac{\mu^2 A^4}{64\omega^2}.$$

From Eq. (8), the stability boundaries of the synchronization are to be found around the two main parametric resonances defined at $a_0 = n^2$ ($n = 1,2$). Floquet theory [24,25] states that η_i may decay to zero or grow to infinity, and therefore decide the behavior of the independent Fourier modes ρ_i [23,26]. Consequently, the stability of each ρ_i depends on the coupling coefficient K and we need to determine the range of K for the synchronization process to be achieved. Thereby, we use the Whittaker method [24] to discuss the unstable solutions. Thus we assume that at the nth unstable region, each solution of Eqs. (8) has the form

$$\eta_i = e^{\alpha_i\tau}\sin(n\tau - \sigma), \tag{9}$$

with α_i being the characteristic exponents and σ a parameter. Substituting Eqs. (9) into Eqs. (8) and equating the coefficient of $\cos n\tau$ and $\sin n\tau$ separately to zero, we find that the characteristic exponents have the following expressions:

$$\alpha_i^2 = -(a_{0i}+n^2) + \sqrt{4n^2 a_{0i} + a_n^2}, \tag{10}$$

with $a_n^2 = a_{ns}^2 + a_{nc}^2$. The synchronization process is stable when the Fourier modes ρ_i go to zero with increasing time, so that the real part of $-\lambda \pm \alpha_i$ should be negative. Since λ is real and positive, the stability condition is reduced to $\lambda^2 > \alpha_i^2$. Consequently, from the relations (7), the synchronization process is stable under the conditions

$$H_i^n = (a_{0i}-n^2)^2 + 2(a_{0i}+n^2)\lambda^2 + \lambda^4 - a_n^2 > 0, \quad n = 1,2. \tag{11}$$

We note that in the second main parametric resonance (i.e., for $n=2$), the conditions (11) are satisfied for all value of i. Thus the stability is analyzed in the first main parametric resonance (i.e., for $n=1$) and H_i^1 helps us to determine the synchronization domain and the stability boundaries. We can now analyze through H_i^1 what happens in the ring when the coupling strength K increases from -0.25 to infinity. It should be noticed that H_1^1 does not depend on the coupling strength. When $K=0$, the system is uncoupled and the Fourier modes ρ_2, ρ_3, and ρ_4 degenerate into ρ_1, which is stable (since it remains bounded as t tends to infinity). Then, the model belongs to the stability area. As K increases, our investigation shows that both H_2^1 and H_3^1 are positive for $K \in]-0.25;-0.0011] \cup [0.004;+\infty[$ while H_4^1 is positive for the range defined as $K \in]-0.25;-0.0006] \cup [0.002;+\infty[$. We can thus discern three domains as follows:

$$I_{1a} =]-0.25;-0.0011] \cup [0.004;+\infty[,$$

$$I_{2a} =]-0.0011;-0.0006] \cup [0.0020;0.004[,$$

$$I_{3a} =]-0.0006;0[\cup]0;0.0020[.$$

When $K \in I_{1a}$, the three modes ρ_2, ρ_3, and ρ_4 are together in the stability domain and thus tend all to zero as the time

increases. Thus the ring is in the complete synchronization state where we have the constraint

$$x_1 = x_2 = x_3 = x_4. \tag{12}$$

In this case, all four oscillators display the same dynamics (e.g., are phase-locked).

For $K \in I_{2a}$, only the fastest mode ρ_4 reaches the stability domain and the ring satisfies the constraint

$$x_4 - x_3 + x_2 - x_1 \equiv 0, \tag{13}$$

while we have

$$x_1 \neq x_3,$$

$$x_2 \neq x_4 \tag{14}$$

since ρ_2 and ρ_3 remain in the unstable domain. This corresponds to what can be called a standard correlated state (SCS).

For $K \in I_{3a}$, the modes ρ_2, ρ_3, and ρ_4 enter into the instability domain. This means that the ring satisfies the following constraint:

$$x_1 \neq x_3,$$

$$x_2 \neq x_4, \tag{15}$$

and

$$x_4 - x_3 + x_2 - x_1 \neq 0. \tag{16}$$

In this case, there is no synchronization in the ring.

B. Results of the numerical simulation

We use the numerical simulation to check the validity and complement the analytical results obtained from Eqs. (11). The numerical simulation uses the fourth-order Runge-Kutta algorithm with a time step $\Delta t = 0.01$ and the initial conditions $(x_1(0);\dot{x}_1(0)) = (1.0;1.0)$, $(x_2(0);\dot{x}_2(0)) = (1.5;1.5)$, $(x_3(0);\dot{x}_3(0)) = (2.0;2.0)$, and $(x_4(0);\dot{x}_4(0)) = (3.0;3.0)$.

Let us evaluate the final values of ρ_i and thus indicate various areas of K where synchronization is achieved. The ring is considered synchronized if each ρ_i vanishes with the precision 10^{-4}. For a fixed value of K in each area I_{ja} $(j = 1,2,3)$, we have plotted the behavior of ρ_k $(k = 2,3,4)$ versus the time in Fig. 3 to show how they look when there is synchronization, when there is no synchronization, and when there is instability.

From the numerical simulation of Eq. (2), complete synchronization occurs for $K \in I_{1n} = [-0.2363; -0.0017] \cup [0.0037; +\infty[$. The system is in the SCS for $K \in I_{2n} =]-0.0011; -0.0009] \cup [0.0029; 0.0037[$. This is due to the fact that $\rho_4 = 0$ while $\rho_2 \neq 0$ and $\rho_3 \neq 0$. For the region of K defined as $K \in I_{3n} =]-0.0009; 0[\cup]0; 0.0029[$, there is no synchronization in the ring because $\rho_2 \neq 0$, $\rho_3 \neq 0$, and $\rho_4 \neq 0$. Two clusters also come from this numerical analysis which do not appear from the analytical investigations. The first one is defined for $K \in [-0.25; -0.2364]$, where $\rho_2 = \rho_3 = 0$, $\rho_4 \neq 0$ corresponding to the state $x_4 = x_2$ and x_3

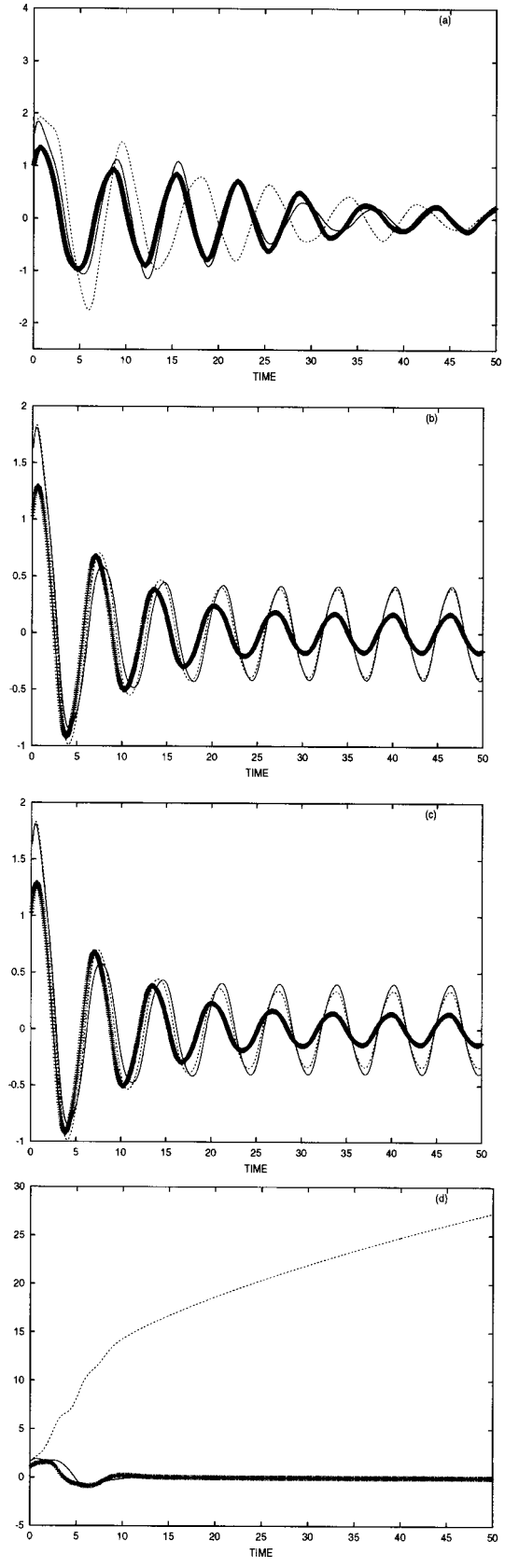

FIG. 3. Temporal variation of the Fourier modes ρ_i with $\mu = 0.10$: (a) $K = -0.10$, (b) $K = -0.0008$, (c) $K = 0.0010$, and (d) $K = -0.26$. ρ_2 (lines), ρ_3 (line points), and ρ_4 (dashed lines).

$=x_1$ with $x_4-x_3+x_2-x_1\neq 0$. The second cluster is for $K \in [-0.0016;-0.0011]$ since $\rho_2\neq 0$ and $\rho_3=\rho_4=0$. It corresponds to $x_1=x_3$ and $x_4+x_2=x_1+x_3$.

IV. INFLUENCE OF THE LOCAL INJECTION

As we have mentioned before, different dynamical states are observed in several identical coupled oscillators such as clustering or complete synchronization. However, sometimes, due to environmental constraints or because of its potential application, the system can be coupled to an external independent oscillator or excitation. This is commonly achieved through the local injection technique consisting of a unidirectional coupling between the external command oscillator and a fixed representative of the nonlinear coupled system [27]. This local injection scheme is sometimes indispensable for the description of undesirable parasite couplings or external perturbations. For example, in the case where external perturbation is the noise, it plays a dual role if applied to a synchronized system. Depending on the system's parameter, the noise can disrupt synchronization or produce a new ordered state whose coherence depends resonantly on the noise intensity. For instance, there is an optimal value of noise intensity which produces maximally regular biperiodic oscillations, and thus coherence resonance [28]. Local injection can also be willingly introduced to force the nonlinear system to replicate the dynamics of the external master oscillator. For instance, in the chaotic oscillators, the local injection method can enable us to recover a particular chaotic orbit when the unidirectional command coupling is suitably designed [9].

When the local injection is taken into account, Eqs. (2) become

$$\ddot{x}_1-\mu(1-x_1^2)\dot{x}_1+x_1=K(x_2-2x_1+x_4)-\Gamma(x_1-x_s),$$

$$\ddot{x}_2-\mu(1-x_2^2)\dot{x}_2+x_2=K(x_3-2x_2+x_1),$$

$$\ddot{x}_3-\mu(1-x_3^2)\dot{x}_3+x_3=K(x_4-2x_3+x_2),$$

$$\ddot{x}_4-\mu(1-x_4^2)\dot{x}_4+x_4=K(x_1-2x_4+x_3), \qquad (17)$$

where x_s represents the dynamics of the external oscillator and also plays the role of the command signal, and Γ is the local injection strength. Generally, the literature places emphasis upon the control of the coupled system to the trivial equilibrium state ($x_s=0$). Even for this simple target, further simplifications are often imposed for the analytical results to be derived. For example, to be sure that the first oscillator can be pinned to the target state $x_s=0$, Γ should be directly set to infinity. Throughout our study, we take x_s as the periodic solution of a Van der Pol equation. Then we have

$$\ddot{x}_s-\mu(1-x_s^2)\dot{x}_s+x_s=0. \qquad (18)$$

Let us rewrite the first-order perturbation equations (3) as follows:

$$\ddot{\xi}_1-\mu(1-x_s^2)\dot{\xi}_1+(1+2\mu x_s\dot{x}_s)\xi_1=K(\xi_2-2\xi_1+\xi_4)-\Gamma\xi_1,$$

$$\ddot{\xi}_2-\mu(1-x_s^2)\dot{\xi}_2+(1+2\mu x_s\dot{x}_s)\xi_2=K(\xi_3-2\xi_2+\xi_1),$$

$$\ddot{\xi}_3-\mu(1-x_s^2)\dot{\xi}_3+(1+2\mu x_s\dot{x}_s)\xi_3=K(\xi_4-2\xi_3+\xi_2),$$

$$\ddot{\xi}_4-\mu(1-x_s^2)\dot{\xi}_4+(1+2\mu x_s\dot{x}_s)\xi_4=K(\xi_1-2\xi_4+\xi_3) \qquad (19)$$

with the deviation $\xi_\nu=x_\nu-x_s$. Following the analysis of Sec. III, Eqs. (19) may now be written under the form of a set of coupled Hill's equations:

$$\ddot{\eta}_1+(a_{01}+2a_{1s}\sin 2\tau+2a_{1c}\cos 2\tau+2a_{2c}\cos 4\tau)\eta_1=\frac{1}{\omega^2}[K(\eta_2-2\eta_1+\eta_4)-\Gamma\eta_1],$$

$$\ddot{\eta}_2+(a_{01}+2a_{1s}\sin 2\tau+2a_{1c}\cos 2\tau+2a_{2c}\cos 4\tau)\eta_2=\frac{1}{\omega^2}[K(\eta_3-2\eta_2+\eta_1)],$$

$$\ddot{\eta}_3+(a_{01}+2a_{1s}\sin 2\tau+2a_{1c}\cos 2\tau+2a_{2c}\cos 4\tau)\eta_3=\frac{1}{\omega^2}[K(\eta_4-2\eta_3+\eta_2)],$$

$$\ddot{\eta}_4+(a_{01}+2a_{1s}\sin 2\tau+2a_{1c}\cos 2\tau+2a_{2c}\cos 4\tau)\eta_4=\frac{1}{\omega^2}[K(\eta_1-2\eta_4+\eta_3)], \qquad (20)$$

where

$$\xi_\nu=\eta_\nu\exp(-\lambda\tau)\exp\left(-\frac{1}{2}\int F(\tau')d\tau'\right), \quad \nu=1,2,3,4.$$

Let us investigate the stability of the synchronization process in the ring. We assume that each solution of Eqs. (20) has the expression

$$\eta_\nu=C_\nu e^{S\tau}\sin(n\tau-\sigma), \qquad (21)$$

where S is the characteristic exponent and C_ν are arbitrary constants. Substituting the solutions η_ν into Eqs. (20) and equating the coefficients of $\sin n\tau$ and $\cos n\tau$ separately to zero gives us the following set of algebraic equations in C_ν:

$$[(S^2-n^2+\delta-a_{nc})\cos\sigma+(2nS-a_{ns})\sin\sigma]C_1-\frac{K}{\omega^2}\cos\sigma C_2-\frac{K}{\omega^2}\cos\sigma C_4=0,$$

$$[(2nS+a_{ns})\cos\sigma-(S^2-n^2+\delta+a_{nc})\sin\sigma]C_1+\frac{K}{\omega^2}\sin\sigma C_2+\frac{K}{\omega^2}\sin\sigma C_4=0,$$

$$-\frac{K}{\omega^2}\cos\sigma C_1+[(S^2-n^2+a_{02}-a_{nc})\cos\sigma+(2nS-a_{ns})\sin\sigma]C_2-\frac{K}{\omega^2}\cos\sigma C_3=0,$$

$$\frac{K}{\omega^2}\sin\sigma C_1+[(2nS+a_{ns})\cos\sigma-(S^2-n^2+a_{02}+a_{nc})\sin\sigma]C_2+\frac{K}{\omega^2}\sin\sigma C_3=0,$$

$$-\frac{K}{\omega^2}\cos\sigma C_2+[(S^2-n^2+a_{02}-a_{nc})\cos\sigma+(2nS-a_{ns})\sin\sigma]C_3-\frac{K}{\omega^2}\cos\sigma C_4=0,$$

$$\frac{K}{\omega^2}\sin\sigma C_2+[(2nS+a_{ns})\cos\sigma-(S^2-n^2+a_{02}+a_{nc})\sin\sigma]C_3+\frac{K}{\omega^2}\sin\sigma C_4=0,$$

$$-\frac{K}{\omega^2}\cos\sigma C_1-\frac{K}{\omega^2}\cos\sigma C_3+[(S^2-n^2+a_{02}-a_{ac})\cos\sigma+(2nS-a_{ns})\sin\sigma]C_4=0,$$

$$\frac{K}{\omega^2}\sin\sigma C_1+\frac{K}{\omega^2}\sin\sigma C_3+[(2nS+a_{ns})\cos\sigma-(S^2-n^2+a_{02}+a_{nc})\sin\sigma]C_4=0. \tag{22}$$

Upon elimination of C_1, C_2, C_3, C_4, and σ in Eqs. (22), we have

$$\Delta_n(S)\equiv\begin{vmatrix}\Delta_{11}&\Delta_{12}&\Delta_{13}&0&0&0&\Delta_{17}&0\\ \Delta_{21}&\Delta_{22}&0&\Delta_{24}&0&0&0&\Delta_{28}\\ \Delta_{31}&0&\Delta_{33}&\Delta_{34}&\Delta_{35}&0&0&0\\ 0&\Delta_{42}&\Delta_{43}&\Delta_{44}&0&\Delta_{46}&0&0\\ 0&0&\Delta_{53}&0&\Delta_{55}&\Delta_{56}&\Delta_{57}&0\\ 0&0&0&\Delta_{64}&\Delta_{65}&\Delta_{66}&0&\Delta_{68}\\ \Delta_{71}&0&0&0&\Delta_{75}&0&\Delta_{77}&\Delta_{78}\\ 0&\Delta_{82}&0&0&0&\Delta_{86}&\Delta_{87}&\Delta_{88}\end{vmatrix}=0, \tag{23}$$

with $n=1$ or $n=2$ and the parameters Δ_{lm} $(l,m=1,2,3,4,5,6,7,8)$ are given by the following expressions:

$$\Delta_{11}=S^2+\Theta_n,\quad \Delta_{22}=-(S^2+\Xi_n),\quad \Delta_{33}=\Delta_{55}=\Delta_{77}=S^2+\Upsilon_n,$$

$$\Delta_{44}=\Delta_{66}=\Delta_{88}=-(S^2+\Psi_n),\quad \Delta_{12}=\Delta_{34}=\Delta_{56}=\Delta_{78}=2nS-a_{ns},$$

$$\Delta_{21}=\Delta_{43}=\Delta_{65}=\Delta_{87}=2nS+a_{ns},$$

$$\Delta_{13}=\Delta_{31}=\Delta_{17}=\Delta_{71}=\Delta_{35}=\Delta_{53}=\Delta_{57}=\Delta_{75}=-\frac{K}{\omega^2},$$

$$\Delta_{24}=\Delta_{42}=\Delta_{28}=\Delta_{82}=\Delta_{46}=\Delta_{64}=\Delta_{68}=\Delta_{86}=\frac{K}{\omega^2},$$

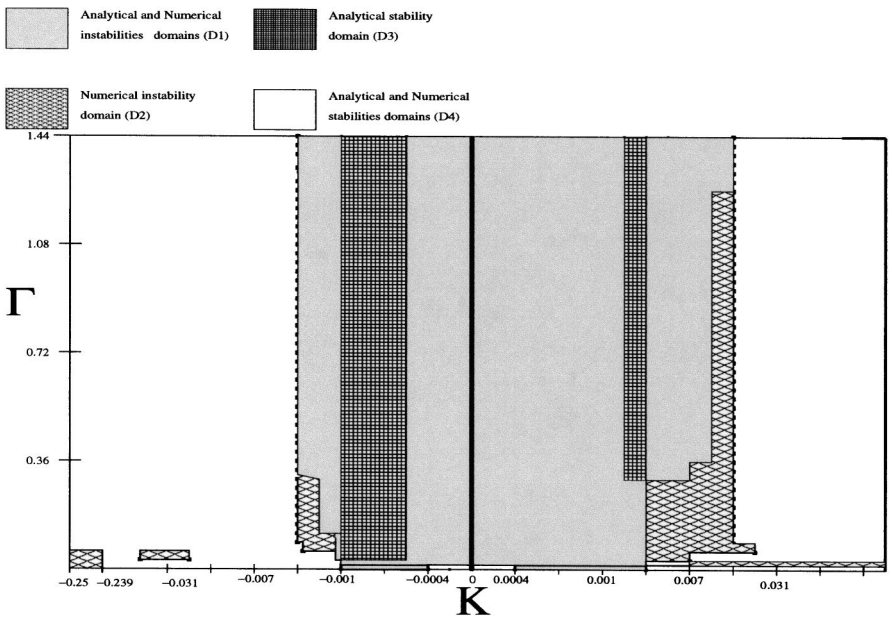

FIG. 4. Stability map.

where

$$\Theta_n = \delta - n^2 - a_{nc}, \quad \Xi_n = \delta - n^2 + a_{nc},$$

$$\Upsilon_n = a_{02} - n^2 - a_{nc},$$

$$\Psi_n = a_{02} - n^2 + a_{nc}, \quad \delta = \frac{2K+\Gamma}{\omega^2} + a_{01},$$

with $n=1$ for $\Delta_1(S)$ and $n=2$ for $\Delta_2(S)$ [see Eq. (23)].

The characteristic exponent S is given by Eq. (23), that is, $\Delta_n(S)=0$. Since the stability condition is given by $\lambda^2 - S^2 > 0$ when assuming that $\lambda > 0$, we have

$$\Delta_n(\lambda) = 0 \tag{24}$$

at the boundary of the nth unstable domain.

In the second main resonance, $\Delta_2(\lambda)$ is positive and does not change its sign. Accordingly, the stability analysis is reduced once more around the first unstable region. Thus, when $\Gamma=0$, our analytical investigation shows that the synchronization process is stable for the range of K defined as $]-0.25;-0.001[\cup]-0.003;0[\cup]0;0.0004[\cup]0.0039;+\infty[$, which is comparable with the interval I_{1a}. Analyzing the effects of the local injection strength on the stability boundary of the ring, we find two ranges as Γ varies. The first range is defined as $0<\Gamma\leqslant 1.5$, where the stability of the ring depends on the local injection strength Γ. For example, when $\Gamma=0.06$, the synchronization process is achieved if $K\in]-0.25;-0.0012[\cup]-0.0011;-0.0006[\cup]0.0039;+\infty[$ and becomes $]-0.25;-0.0035[\cup]-0.0011;-0.0006[\cup]0.0023;0.0040[\cup[0.0110;+\infty[$ when Γ is 0.6. In the second range, i.e., $\Gamma\in]1.5;+\infty[$, we find that the stability domain of the synchronization does not change with the variation of the local injection strength and is defined as $K\in]-0.25;-0.0036[\cup]-0.0011;-0.0006[\cup]0.0023;0.0040[\cup]0.0133;+\infty[$. To confirm the validity of our analytic investigation, we have solved numerically Eqs. (17) with the fourth-order Runge-Kutta algorithm. Synchronization between two oscillators p and q occurs with a criterion that the distance of the phase trajectories be

$$d_{pq} = |x_p - x_q| < h, \tag{25}$$

where $h=10^{-3}$ is the precision. Synchronization among all the oscillators occurs if the total separation of all pairs of trajectories is smaller than an accuracy, namely

$$d = \sum_{\text{pairs}(pq)} d_{pq} < h. \tag{26}$$

For higher accuracy (with a smaller h), computational time has been extended to 10^5. In Fig. 4, we show the stability map by applying the numerical simulation of the equation of motion (17) and the preceding analytical investigation. The resulting synchronized states in the (K,Γ) plane are drawn for a fixed value of the injection strength Γ when the coupling parameter K varies. The following results are observed.

The map shows four different areas: (D_1), (D_2), (D_3), and (D_4) (see Fig. 4). The intersection between both analytical and numerical instability areas corresponds to (D_1), while (D_4) is the intersection between the analytical and the numerical stability areas. As for (D_2), it shows the instability domain that is not predicted analytically while (D_3) is the stability domain forecasted analytically but not numerically. As Γ increases, both analytical and numerical instability areas become closer. For example, when $\Gamma=0.06$, the numerical simulation gives that the synchronization is unstable for $K\in[-0.25;-0.241]\cup[-0.003;0[\cup]0;0.021]$ and becomes $[-0.004;0[\cup]0;0.013]$ when $\Gamma=0.60$. The existence of clusters in the numerical instability domain (D_2) should be noted since, to obtain complete synchronization, all the clusters should be synchronized between them. This phenomenon $(\rho_2=0)$ can be displayed, for example, when

$\Gamma = 0.03$ in the interval $[-0.25; -0.239]$. When $\Gamma > 1.44$, the map configuration remains unchanged. It is important to remark that (D_1) and (D_4) are two regions where the agreement between analytical and numerical results is quite good.

It is also clear throughout our analytic investigation that, in opposition to the case where the coupled system is studied around the trivial equilibrium state $x_s = 0$ and for which we need to set directly Γ to infinity to assure the synchronization, it is not necessary when $x_s \neq 0$.

V. CONCLUSION

In this paper, we have studied the stability of the synchronization in a ring of mutually coupled self-sustained oscillators with and without a local injection. The Whittaker method has permitted us to obtain the boundaries of the synchronization process when the local injection is not present. When we take into account the local injection effect, the same analytical method helps us to obtain a stability map for complete synchronization to the external excitation.

As noted in the Introduction, the model analyzed in this paper is a representative of many systems. We think that following the preliminary results obtained here, a close inspection of the realistic models in the context of physics, biology, and electronics is still an interesting task. Indeed, coming back to the electronic system shown in Fig. 1, it should be stressed that when K belongs to I_{1n}, all four microwave oscillators are phase-locked. Thus the wave signal emitted appears to be more powerful. The state where $x_1 = x_3$ and $x_2 = x_4$ is also interesting since it corresponds to the situation where two microwave oscillators are phase-locked one after the other with possible implications in automation engineering.

ACKNOWLEDGMENT

The authors thank T. Endo for enriching contributions.

APPENDIX

When the N electrical oscillators are interconnected, the νth oscillator is described by the following equations:

$$V_\nu - V_{\nu+1} = L_c \frac{dI_\nu}{d\tau}, \tag{A1}$$

$$I_{\nu-1} - I_\nu = i_L + i_C + i_\nu = \frac{1}{L}\int V_\nu d\tau - C\frac{dV_\nu}{d\tau} - a_1 V_\nu + a_3 V_\nu^3. \tag{A2}$$

The first time derivative of Eq. (A2) leads us to

$$\frac{dI_{\nu-1}}{d\tau} - \frac{dI_\nu}{d\tau} = \frac{1}{L}V_\nu - C\frac{d^2V_\nu}{d\tau^2} - a_1\frac{dV_\nu}{d\tau} + 3a_3V_\nu^2\frac{dV_\nu}{d\tau}. \tag{A3}$$

Then using Eq. (A1), we obtain that the voltage in the capacitor of the νth oscillator obeys the equation

$$\frac{1}{L_c}(V_{\nu-1} - V_\nu) - \frac{1}{L_c}(V_\nu - V_{\nu+1}) = \frac{1}{L}V_\nu + C\frac{d^2V_\nu}{d\tau^2} - a_1\left(1 - 3\frac{a_3}{a_1}V_\nu^2\right)\frac{dV_\nu}{d\tau}. \tag{A4}$$

This latter equation can be rewritten as follows:

$$\frac{d^2V_\nu}{d\tau^2} - \frac{a_1}{C}\left(1 - 3\frac{a_3}{a_1}V_\nu^2\right)\frac{dV_\nu}{d\tau} + \frac{1}{LC}V_\nu = \frac{1}{L_cC}(V_{\nu-1} - 2V_\nu + V_{\nu+1}). \tag{A5}$$

The substitution of the quantities

$$w_e^2 = \frac{1}{LC}, \quad t = w_e\tau, \quad V_\nu = \sqrt{\frac{a_1}{3a_3}}x_\nu$$

gives the set of Eqs. (2) with

$$\mu = a_1\sqrt{\frac{L}{C}}, \quad K = \frac{L}{L_c}.$$

[1] L. M. Pecora, T. L. Carroll, G. A. Johnson, and D. J. Mar, Chaos **7**, 520 (1997).
[2] S. Nakata, T. Miyata, N. Ojima, and K. Yoshikawa, Physica D **115**, 313 (1998).
[3] K. Miyakawa and K. Yamada, Physica D **151**, 217 (2001).
[4] R. E. Mirollo and S. H. Strogatz, SIAM (Soc. Ind. Appl. Math.) J. Appl. Math. **50**, 1645 (1990).
[5] S. H. Strogatz and I. Stewart, Sci. Am. (Int. Ed.) **68**, 102 (1993).
[6] Y. Kuramoto, *Chemical Oscillations, Waves and Turbulence* (Springer, Berlin, 1984).
[7] P. Reimann, C. Van den Broeck, and R. Kawai, Phys. Rev. E **60**, 6402 (1999).
[8] Y. Zhang, G. Hu, H. A. Cerdeira, S. Chen, T. Braun, and Y. Yao, Phys. Rev. E **63**, 026211 (2001).
[9] Y. Chembo Kouomou and P. Woafo, Phys. Rev. E **66**, 066201 (2002).
[10] Y. Chembo Kouomou and P. Woafo, Phys. Rev. E **67**, 046205 (2003).
[11] D. Somers and N. Kopell, Biol. Cybern. **68**, 393 (1993).
[12] D. Somers and N. Kopell, Physica D **89**, 169 (1995).
[13] T. Ookawara and T. Endo, IEEE Trans. Circuits Syst., I: Fundam. Theory Appl. **46**, 827 (1999).
[14] B. Van der Pol, Philos. Mag. **43**, 700 (1922).
[15] B. Van der Pol, Proc. IRE **22**, 1051 (1934).
[16] K. Fukui and S. Nogi, IEEE Trans. Microwave Theory Tech. **28**, 1059 (1980).
[17] K. Fukui and S. Nogi, IEEE Trans. Microwave Theory Tech.

34, 943 (1986).
[18] T. Endo and S. Mori, IEEE Trans. Circuits Syst. **23**, 100 (1976).
[19] B. Robertson-Dunn and D. A. Linkens, J. Med. Biol. Eng. **12**, 750 (1974).
[20] D. A. Linkens, IEEE Trans. Biomed. Eng. **23**, 101 (1976).
[21] J. D. Murray, *Mathematical Biology* (Springer, New York, 1989).
[22] T. Endo and S. Mori, IEEE Trans. Circuits Syst. **25**, 7 (1978).
[23] P. Woafo and R. A. Kraenkel, Phys. Rev. E **65**, 036225 (2002).
[24] C. Hayashi, *Nonlinear Oscillations in Physical Systems* (McGraw Hill, New York, 1964).
[25] A. H. Nayfeh and D. T. Mook, *Nonlinear Oscillations* (Wiley-Interscience, New York, 1964).
[26] Y. Chembo Kouomou and P. Woafo, Phys. Lett. A **298**, 18 (2002).
[27] G. Hu, J. Xiao, J. Gao, X. Lie, Y. Yao, and H. Bambi, Phys. Rev. E **62**, R3043 (2000).
[28] A. G. Balanov, N. B. Janson, D. E. Postnov, and P. V. E. McClintock, Phys. Rev. E **65**, 041105 (2002).